

# Cells tracking in a live zebrafish embryo

Camilo Melani, Matteo Campana, Benoit Lombardot, Barbara Rizzi, Federico Veronesi, Cecilia Zanella, Paul Bourguine, Karol Mikula, Nadine Peyri ras and Alessandro Sarti

**Abstract**— We designed a set of procedures for achieving the tracking of cell nuclei and the identification of cell divisions in live zebrafish embryos using 3D+time images acquired by confocal laser scanning microscopy (CLSM). Our strategy includes image signal enhancement with feature preserving denoising algorithm, automated identification of the nuclei position, extraction of the optical flow from 3D images sequences and tracking of nuclei.

## I. INTRODUCTION

Understanding the cell morphodynamics underlying morphogenetic processes is a fundamental issue for bio-medical research. Such a goal can be achieved through the automated tracking of cell nuclei and cell divisions from 3D+time *in vivo* imaging [1]. These tasks are the basis for the reconstruction of the cell lineage tree described as the branching process of cell divisions and its deployment in space and time. The complete reconstruction of the cell lineage tree from the egg cell to the adult stage has only been achieved for the worm *Caenorhabditis elegans*. However, in that case, the total cell number in the adult is less than one thousand and the cell lineage is largely invariant. Because of their very large cell number, this challenge has not been taken up so far for vertebrate organisms. Nevertheless, recent advances in imaging strategies open the way to *in toto* 3D plus time imaging providing data suitable for *in vivo* cell tracking and cell morphodynamics reconstruction. The zebrafish (*Danio rerio*) is a vertebrate model that has been chosen for its transparency allowing *in vivo* inspection at the cellular level deep into the tissues by confocal laser scanning microscopy [2]. The zebrafish exhibits typical vertebrate differentiated cell types and has been largely validated for investigations related to humans including cancerogenesis and a number

This work was supported by the European projects *Computer Vision Foundations and Applications* (Alfa II-0366-FA), *Embryomics* (NEST 012916) and *BioEmergences* (NEST 028892)

C.Melani is with Facultad de Ciencias Exactas y Naturales, Universidad de Buenos Aires, Argentina and Dipartimento di Elettronica, Informatica e Sistemistica, Universit  di Bologna, Italy. [camilo@dc.uba.ar](mailto:camilo@dc.uba.ar)

N.Peyri ras is with DEPSN, Centre National De La Recherche Scientifique (CNRS), Institut de Neurobiologie Alfred Fessard, Gif-sur-Yvette, France. [nadine.peyrieras@inaf.cnrs-gif.fr](mailto:nadine.peyrieras@inaf.cnrs-gif.fr)

K.Mikula is with Dept. of Mathematics and Descriptive Geometry, Slovak University of Technology, Slovakia. [mikula@math.sk](mailto:mikula@math.sk)

C.Zanella M.Campana, B.Rizzi, F.Veronesi and A.Sarti are with Dipar. di Elettronica, Informatica e Sistemistica, Universit  di Bologna, Italy. [cecilia.zanella2@unibo.it](mailto:cecilia.zanella2@unibo.it) [[mcampana](mailto:mcampana), [brizzi](mailto:brizzi), [fveronesi](mailto:fveronesi), [asarti](mailto:asarti)][@deis.unibo.it](mailto:deis.unibo.it)

B.Lombardot and P.Bourguine are with Centre de Recherche en Epist mologie Appliqu e, CNRS  cole Polytechnique, Paris, France. [benoit.lombardot@espci.org](mailto:benoit.lombardot@espci.org), [bourguine@shs.polytechnique.fr](mailto:bourguine@shs.polytechnique.fr)

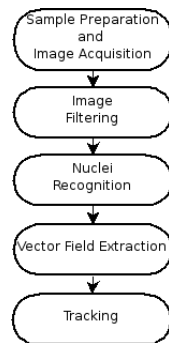


Fig. 1. Workflow showing the data reconstruction steps to estimate the cells position and movements: 3D+time images acquisition; the noise level reduction and relevant information extraction.

of genetic diseases [3]. Achieving the automated reconstruction of the zebrafish embryo cell morphodynamics is highly relevant for investigating stem cells populations, early steps of cancerogenesis or drug effects *in vivo*. Such a goal requires engineering live zebrafish embryos to highlight sub-cellular structures to be imaged by time lapse laser scanning microscopy, designing image processing algorithms and computational methods. We define in this paper a set of algorithms to identify the 3D location of cell nuclei, estimate cell movements and identify cell divisions. The workflow is summarized in Fig. 1.

The rest of the paper is organized as follows: Section II briefly explains the image acquisition method. Section III introduces a nonlinear edge-preserving filtering method used to increase the signal to noise ratio in 3D images. Section IV shows how a fully automated method identifying spheres in 3D images can be used to recognize nuclei. In Section V, we examine a procedure based on level-sets methods to estimate the movements of cells. Section VI explains the tracking procedure and detection of cell divisions.

## II. IMAGE ACQUISITION

Zebrafish embryos have been labelled through injection at the one cell stage of RNAs encoding *farnesylated mcherry* fluorescent protein (membrane staining) and histone *H2B/eGFP* fusion protein (nuclei staining) respectively. That staining produces very high contrast images containing high intensity membrane (nucleus) regions versus low intensity regions without membranes (nuclei). The image data set used in this paper to design and validate our reconstruction strategy has been obtained by confocal laser scanning microscopy with a SP2 Leica upright microscope with a 40x/0.8NA water objective and 488nm and 561nm laser light excitation.

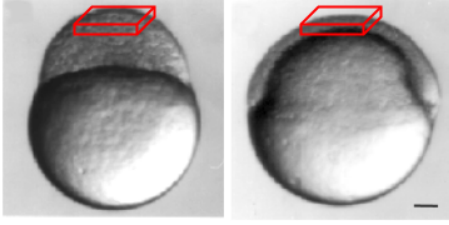


Fig. 2. Zebrafish embryo. Scale bar: 100  $\mu\text{m}$ . The boxes represent the region of the embryo obtained by confocal laser scanning microscopy. Left: embryo at 3.5 hours post fertilization. Right: embryo at 7.5 hours post fertilization.

2D images are acquired parallel to the focal plane  $xy$ . The images size is (512 x 512) pixels (8 bits per pixel). Images are taken at regularly spaced  $z$  depth in the specimen to build a  $z$  stack. The number of section in each volume is 30. The voxel size is (0,58 x 0,58 x 1)  $\mu\text{m}$ . Repeating this procedure through time generates a sequence of 3D images. The 49 volumes have been taken every 5 minutes from 3.5hpf (hours post fertilization at 28°C) for 4 hours (at 25°C) from the animal pole (Fig. 2) [4].

### III. FILTERING

Image enhancement and denoising is a critical step in order to preserve the shape information in digital images. Furthermore, in laser scanning microscopy imaging, noise is due to different causes, and is difficult to model. In particular, the variation of the fluorescent molecules concentration (synthesized from the injected RNA) superimposes a de facto noise level that is difficult to model. The use of traditional preprocessing algorithms (moving average, median and Gaussian filtering) do reduce the noise superimposed on the image but do not maintain a good definition of the edges or image features. The goal of the filtering process is to reduce the noise from the images without losing useful details like the edges. For that reason we have been using a noise removal method based on the Perona and Malik anisotropic diffusion filter [5]. This filter can be viewed as a diffusion process that favours intra-region smoothing while inhibiting inter-region smoothing. A 3D image can be represented by a function  $I : D_I \rightarrow T$  where  $D_I$  is a subset of  $\mathbb{Z}^3$  and  $T$  is an ordered set of grey-level values. The filtered 3D volume is the solution of a nonlinear diffusion equation (1) with the original 3D volume  $I_0$  as initial condition and reflecting boundary conditions.

$$I_t(\bar{x}, t) = \text{div} (g(|\nabla I(\bar{x}, t)|) \nabla I(\bar{x}, t)) \quad (1)$$

where  $g$  is a simple edge indicator

$$g(|\nabla I(\bar{x}, t)|) = \frac{1}{1 + \left( \frac{\|\nabla I(\bar{x}, t)\|}{K} \right)^2} \quad (2)$$

The edge indicator function  $g$  is a non-increasing function of  $|\nabla I(\bar{x}, t)|$ , thus, the value of  $g$  is closer to 1 in flat areas ( $|\nabla I(\bar{x}, t)| \rightarrow 0$ ) and closer to 0 in areas with large changes in image intensity, i.e. the local edge features. The variable

$K$  is a parameter defining the sensitivity of filtering to the image contrast.

### IV. 3D NUCLEI RECOGNITION

In order to recognize all the cell nuclei in each 3D image with a fully automated procedure we have developed a 3D version of the Hough transform for the identification of spherical shapes. The Hough transform is an algorithm which can be used to isolate features of a particular shape within an image [6]. It is commonly used for the detection of regular curves such as lines, circles or ellipses. The algorithm uses the duality between points on a curve and parameters of that curve.

Before applying the Hough transform, the volumes are transformed into an edge representation using the Canny edge detection algorithm [7] which has mainly three advantages that make it optimal as a preprocessing step of the Hough transform: it is able to locate and mark all real edges, it minimizes the distance between the detected edge and real edge and it produces only one response per edge.

A sphere with center  $(x_0, y_0, z_0)$  and radius  $r$  is the set of points  $(x, y, z)$  where  $(x - x_0)^2 + (y - y_0)^2 + (z - z_0)^2 = r^2$  and the parameter space of the spheres with a fixed radius is a three dimensional space defined by  $(x_0, y_0, z_0)$ . We also know that the center of a sphere is located  $r$  units from the point  $(x, y, z)$  in the direction of the gradient of the image in  $(x, y, z)$ .

The Hough transform accumulates in a 3 dimensional array the votes of the edge points of the image. The coordinates of those votes represent the parameters of the spheres that we are looking for. Therefore, coordinates with the highest value, are most likely representing the parameters of a sphere in the image space. Thus, the set of points  $C = \{c = (x, y, z) : c \text{ is a center of a nucleus}\}$  is defined by the local maximums in the accumulator array.

### V. VECTOR FIELD EXTRACTION

Optical flow techniques have been used to estimate pixel correspondence between images obtained at two different times. Therefore, optical flow can give important information about the movement of the objects in the images [8]. This movement is represented by a vector field  $V : D_I \rightarrow \mathbb{R}^3$ .

The brightness of the cells in the confocal volume of the zebrafish embryo remain almost constant over time, meaning that

$$\frac{dI(\bar{x}, t)}{dt} = 0 \quad (3)$$

Taking the first order Taylor expansion of (3), we obtain the *optical flow constraint* equation:  $\nabla I(\bar{x}, t) \cdot \vec{V} + I_t(\bar{x}, t) = 0$ , where  $\vec{V} = (u, v, w)^T$  is the displacement at  $\bar{x}$ . Therefore the component of the movement in the direction of the image gradient is [9]:

$$V_n = \frac{I_t(\bar{x})}{|\nabla I(\bar{x})|} \quad (4)$$

Then, the *optical flow constraint* just is enough to determine the component of the flow field in the orthogonal

direction of the image gradient but not to retrieve the entire vector field. Vemuri et al. [10] overcame this problem by developing a neat and elegant surface evolution approach to achieve the smooth deformation field between two 3D images expressed in a level-sets framework.

Registering two consecutive 3D images  $I_1$  and  $I_2$  is equivalent to determine the evolution of the level-sets of  $I_1$  along its normal direction  $\nabla I$  until it becomes the target image  $I_2$ . This evolution can be written as:

$$I_t(\bar{x}, t) = S \|\nabla I(\bar{x}, t)\| \quad (5)$$

with  $I(\bar{x}, 0) = I_1(\bar{x})$

where  $S$  is the speed term. Choosing the speed term  $S$  equal to  $I_2(\bar{x}) - I(\bar{x}, t)$  makes this curve evolution stop when the image  $I$  reaches the level-sets of the target image  $I_2$ .

Equation (5) does not give explicitly the transformation vector field between the two images that can be achieved using an analogous surface evolution in vector form:

$$\vec{V}_t = (I_2 - I(\vec{V}(\bar{x}, t))) \frac{\nabla I(\vec{V}(\bar{x}, t))}{\|\nabla I(\vec{V}(\bar{x}, t))\|} \quad (6)$$

with  $\vec{V}(\bar{x}, 0) = \vec{0}$

where  $\vec{V}(\bar{x}) = (x + u, y + v, z + w)$ .

Since the movement of cells in the embryo depends locally on the neighbouring cells, the vector field we are expecting should behave as a fluid deformation. In order to achieve a smooth vector field the images are convolved with a Gaussian kernel  $G_\sigma$  before taking its gradient, therefore, expressions (6) and (5) are modified into:

$$I_t(\bar{x}, t) = (I_2(\bar{x}) - I(\bar{x}, t)) \|\nabla G_\sigma * I(\bar{x}, t)\| \quad (7)$$

with  $I(\bar{x}, 0) = I_1(\bar{x})$  and

$$\vec{V}_t = (I_2 - I(\vec{V}(\bar{x}, t))) \frac{\nabla G_\sigma * I(\vec{V}(\bar{x}, t))}{\|\nabla G_\sigma * I(\vec{V}(\bar{x}, t))\|} \quad (8)$$

with  $\vec{V}(\bar{x}, 0) = \vec{0}$  and the gradient is approximated by using the upwind schemes [9].

## VI. TRACKING

We developed a greedy algorithm able to perform the tracking of nuclei and identify the cell divisions combining the information of the nuclei centers with the optical flow.

A cell lineage tree can be interpreted as a binary tree where the first cell of the embryo is represented by the root node and the relationship of mother cells and the two daughter cells are represented by edges.

The imaging procedure started when the embryo had already more than 1000 cells, thus, we created as many trees as nuclei identified in the first set of images.

The algorithm builds the trace of nuclei sequentially from consecutive frames. It first calculates the sets of nuclei centers  $C_\tau$  and  $C_{\tau+1}$  using the Hough transform and the

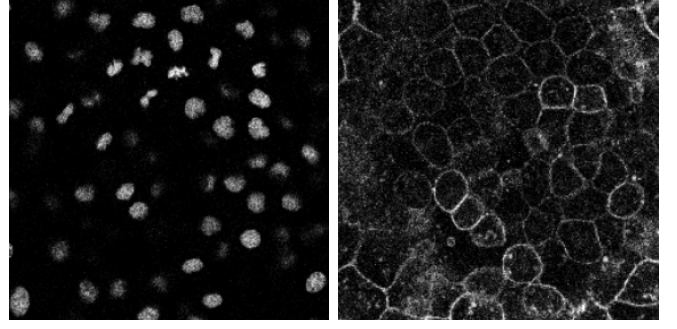


Fig. 3. Section  $xy$  of the 3D volume captured by CLSM in a labelled zebrafish embryo. The embryo is excited with 488nm laser light (left) to reveal the nuclei and excited with 561nm laser light (right) to reveal the membranes.

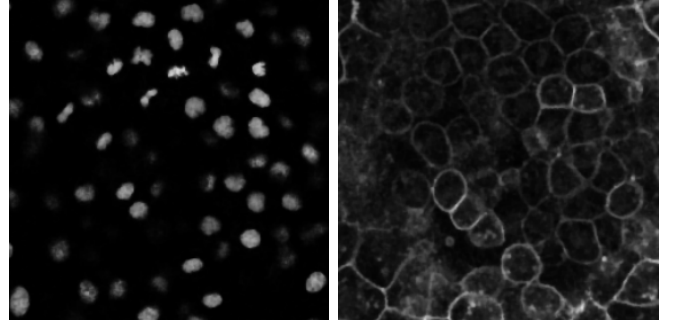


Fig. 4. Denoising procedure. Denoised version of the 3D images shown in Fig. 3 using 4 steps of the anisotropic diffusion filter. Left: nucleus channel. Right: membrane channel.

optical flow  $V_\tau$  from frames  $\tau$  to  $\tau + 1$ . Then it moves each point in  $C_\tau$  with the vector field  $V_\tau$  to build a new set of points  $C'_\tau$ . The points of  $C'_\tau$  are an estimation of the position of the cells in the frame  $\tau + 1$ . At last for each point  $j \in C_{\tau+1}$  the algorithm looks for the nearest point  $i' \in C'_\tau$  and adds the edge  $(i, j)$  to the tree.

A newborn daughter cell is supposed to be really close to the position of its mother, thus, if a cell  $i_\tau$  has two cells  $j_{\tau+1}$  and  $k_{\tau+1}$  as nearest neighbours, this characteristic is recorded in the tree and a cell division is recognized.

## VII. RESULTS

The images acquired by CLSM are shown in Fig. 3 and show labelled membranes or nuclei. The signal found in the nuclei or membranes is not smooth and the images are processed with an anisotropic diffusion filter that reduce noise inside and outside nuclei and membranes preserving the edges information (Fig.4).

The filtered version of nuclei images are treated with the Hough transform to identify the 3D position of nuclei. Visual inspection allows concluding that the procedure leads to a low number of false positive or false negative nuclei detection (Fig. 5). We also observed that the Hough transform successfully detects mitotic (undergoing division) nuclei that are no longer spherical.

In order to capture the cells movement we computed, using the level-sets framework, the optical flow of 3D volumes

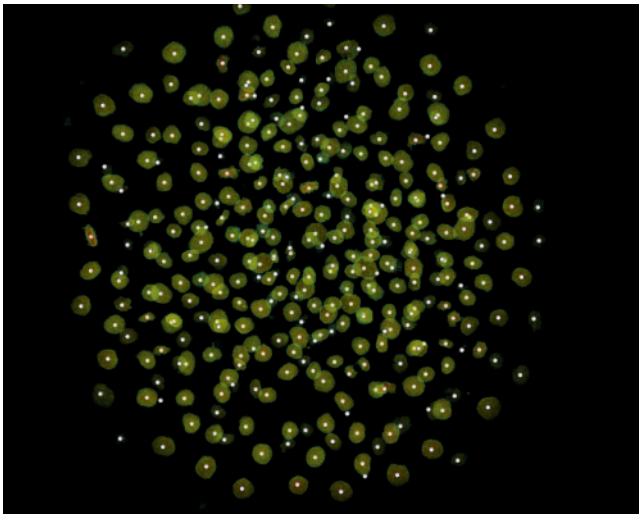


Fig. 5. Nuclei recognition: the 3D images are rendered using a volume ray casting algorithm. A white sphere is rendered everywhere the Hough transform recognizes a nucleus.

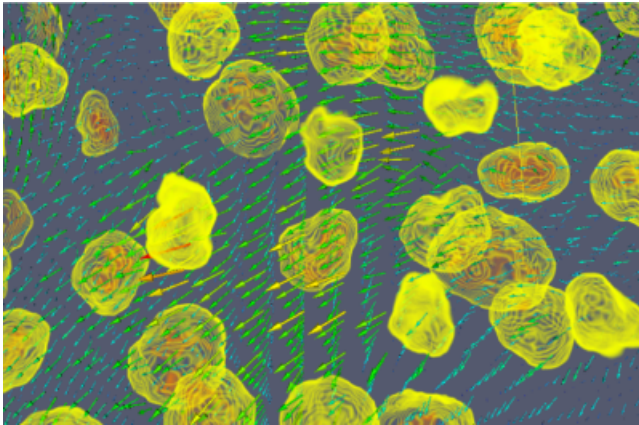


Fig. 6. 3D optical flow of consecutive frames. The vector field represented with coloured arrows is an estimation of the movement of the cells. Parameters: 10 iterations with  $G_\sigma = 4$ .

acquired at consecutive time steps. Fig. 6 shows a portion of the embryo and the vector field calculated with level-sets method.

We used a backtracking procedure to track hundreds of cells, recognize cell divisions and track the relationship between mother and daughter cells (Fig. 7). These results were validated by systematic visual inspection.

### VIII. CONCLUDING REMARKS

We presented a set of procedures to achieve the automated reconstruction of the cell lineage tree in living embryos. These steps include efficient low-level algorithms to filter the 3D confocal images, identify the location of nuclei and estimate the motion of cells in the sequence of images. The nuclei position and the vector field are combined to perform the tracking of cells and identify cell divisions.

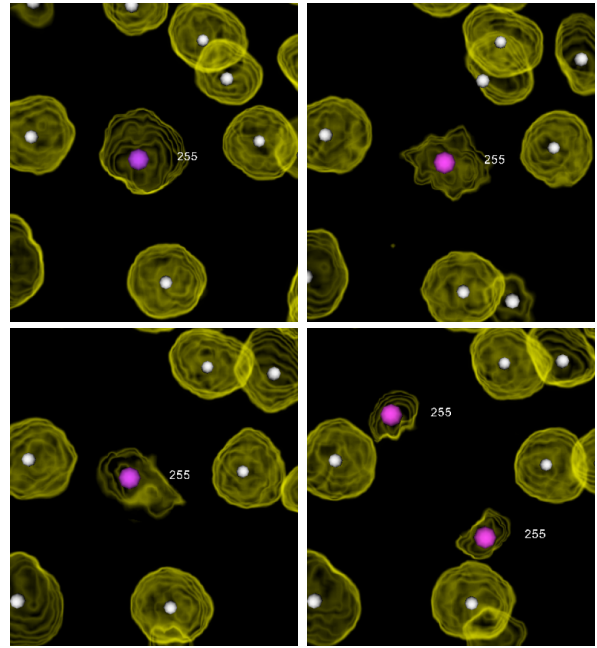


Fig. 7. Tracking result experience. 3D+time images rendered using a volume ray casting algorithm. The time step between frames is 5 minutes. White spheres are rendered everywhere the Hough transform finds a nucleus. A marker (255) shows a cell mitosis. From left to right and top to bottom: prophase, prometaphase, metaphase, telophase.

### IX. ACKNOWLEDGEMENT

We thank all the members of the Embryomics and BioE-mergences projects for our very fruitful interdisciplinary interaction.

### REFERENCES

- [1] S. G. Megason and S. E. Fraser, "Digitizing life at the level of the cell: high-performance laser-scanning microscopy and image analysis for in toto imaging of development." *Mech Dev*, vol. 120, no. 11, pp. 1407–1420, November 2003.
- [2] M. Cooper, L. D'Amico, and C. Henry, "Confocal microscopic analysis of morphogenetic movements," *Methods in Cell Biology*, vol. 59, no. 7, pp. 179–204, 1999.
- [3] K. Dooley and L. Zon, "Zebrafish: a model system for the study of human disease," *Curr Opin Genet Dev*, vol. 10, no. 3, pp. 252–256, Jun 2000.
- [4] C. Kimmel, W. Ballard, S. Kimmel, B. Ullmann, and T. Schilling, "Stages of embryonic development of the zebrafish," *Dev. Dyn.*, vol. 203, pp. 253–310, 1995.
- [5] P. Perona and J. Malik, "Scale-space and edge detection using anisotropic diffusion." *IEEE Trans. Pattern Anal. Mach. Intell.*, vol. 12, no. 7, pp. 629–639, 1990.
- [6] R. O. Duda and P. E. Hart, "Use of the hough transformation to detect lines and curves in pictures." *Commun. ACM*, vol. 15, no. 1, pp. 11–15, 1972.
- [7] J. Canny, "A computational approach to edge detection." *IEEE Trans. Pattern Anal. Mach. Intell.*, vol. 8, no. 6, pp. 679–698, November 1986.
- [8] B. K. Horn and B. G. Schunck, "Determining optical flow." Cambridge, MA, USA, Tech. Rep., 1980.
- [9] J. Sethian, "Level set methods and fast marching methods: Evolving interfaces in computational geometry," 1998.
- [10] B. C. Vemuri, J. Ye, Y. Chen, and C. M. Leonard, "A level-set based approach to image registration." in *MMBIA '00: Proceedings of the IEEE Workshop on Mathematical Methods in Biomedical Image Analysis*. Washington, DC, USA: IEEE Computer Society, 2000, p. 86.